Biosensors and Bioelectronics 25 (2010) 2182–2185

Contents lists available at ScienceDirect

Biosensors and Bioelectronics

journal homepage: www.elsevier.com/locate/bios

Short communication

Gold nanoparticle embedded silicon nanowire biosensor for applications of label-free DNA detection

Seong-Wan Ryu[a], Chang-Hoon Kim[a], Jin-Woo Han[a], Chung-Jin Kim[a], Cheulhee Jung[b], Hyun Gyu Park[b], Yang-Kyu Choi[a,*]

[a] School of Electrical Engineering and Computer Sciences, Division of Electrical Engineering, KAIST, Daejeon 305-701, Republic of Korea
[b] Department of Chemical and Biomolecular Engineering, KAIST, Daejeon 305-701, Republic of Korea

ARTICLE INFO

Article history:
Received 4 December 2009
Received in revised form 28 January 2010
Accepted 15 February 2010
Available online 23 February 2010

Keywords:
Gold nanoparticle
Silicon nanowire
DNA
Oligonucleotide immobilization
Hybridization

ABSTRACT

Gold nanoparticle (GN) embedded silicon nanowire (SiNW) configuration was proposed as a new biosensor for label-free DNA detection to enhance the sensitivity. The electric current flow between two terminals, a source and a drain electrode, were measured to sense the immobilization of probe oligonucleotides and their hybridization with target oligonucleotides. The complementary target oligonucleotide, breast cancer DNA with 1 pM, was sensed. In addition, its sensing mechanism and limit of detection (LOD) enhancement was investigated through simulation. The results support that the LOD can be improved by reducing the SiNW doping concentration. This emerging architecture combined nanostructure of spherical GN and SiNW has high potential as a label-free biosensor due to its facile fabrication process, high thermal stability, immobilization efficiency with a thiol-group in a self-assembled monolayer (SAM), and improved sensitivity.

1. Introduction

Under the needs of specific DNA binding recognition over the areas of genomics, proteomics, biomedical diagnostics, and drug discovery, DNA chips have been implemented in a manner of sensing the modulation factors for a variety of transducers, such as the microbalance (Caruso et al., 1997), surface plasmon resonance (SPR) spectroscopy (Homola et al., 1999), fluorescent assays (Chehab and Kan, 1989), biomechanical cantilever array (Fritz et al., 2000), and electrochemistry (Drummond et al., 2003). Among these transducers, electrochemistry and fluorescence techniques have been developed from the earliest days and are well-established for research and medical treatments due to the their own advantages of simplicity, low cost, and high sensitivity. These techniques are now evolving in connection with modification by gold nanoparticles (GN). In terms of material, gold holds the high biocompatibility and chemical affinity with a thiol-group in a self-assembled monolayer (SAM) to immobilize DNA; hence, it enables an easy binding process and improves binding selectivity compared to the other materials such as silicon (Ohgi et al., 1998). For the nano-structural aspects, a functionalized GN probe to detect oligonucleotides characterized a high binding constant between a target and the probe based on enhanced thermal stability then induced high sensibility (Xu and Craig, 2005; Lytton-Jean and Mirkin, 2005; Akamatsu et al., 2006). Furthermore, GN-bound electrodes showed increased immobilization rates and enhanced hybridization efficiency (Liu et al., 2005; Yang et al., 2007).

Among the label-free DNA detecting platforms including SPR, QCM, the mechanical cantilever array, and silicon nanowire (SiNW), SiNW-based biosensors have been highlighted due to their high scalability, reliability, mass-producibility, and possibility of on-chip integration through highly matured semiconductor technology, referred to as a 'top down' approach (Elfstrom et al., 2008). Furthermore, the configuration of SiNW-based biosensors provides a large surface-to-volume ratio and extends the limit of detection (LOD) as a transducer for label-free, direct, and real-time DNA detection.

To sum up, the GN probes and the SiNW, *i.e.* the combination of each advantage, can bring various benefits in terms of a high binding constant with targets as well as a simple binding process and the feasibility of on-chip integration. However, a mixed approach combining the GN and SiNW techniques has not yet been investigated. It is expected that the mixed approach can provide high sensitivity without additional amplification of the target sequence, such as a polymerase chain reaction (PCR). Therefore, we explore the GN embedded SiNW configuration, which merges the aforementioned techniques as a DNA sensor to achieve sensitivity enhancement for in-vitro diagnostics in this work.

* Corresponding author. Tel.: +82 42 350 3477; fax: +82 42 350 8565.
E-mail address: ykchoi@ee.kaist.ac.kr (Y.-K. Choi).

0956-5663/$ – see front matter © 2010 Elsevier B.V. All rights reserved.
doi:10.1016/j.bios.2010.02.010

2. Experimental

2.1. Fabrication

The GN embedded SiNW devices were fabricated on a silicon-on-insulator (SOI) substrate with a top silicon thickness of 110 nm. The initial doping concentration of the top silicon was 1×10^{15} cm^{-3}. The top silicon was thinned down to 80 nm by thermal oxidation and a wet removal process. The photoresist with a line width of 150 nm was defined by a KrF lithography tool, and thereafter the photoresist was partially trimmed down to a line width of 80 nm by O_2 plasma ashing process (Asano et al., 2001). The dry etch process was applied to pattern the top silicon. Then, the dimension of the nanowire with a width of 80 nm and a height of 80 nm was reduced to 50 nm through iterative oxidation and wet-etching by buffered-oxide-etchant (NH_4F + HF). The two ends of the nanowire are connected to the large pad area in order to provide a measurable contact size. These pads firmly clamp onto the SiNW as well. The nanowire length, defined as the distance between two pads, is 500 nm. To form the GNs on the prepared one-dimensional SiNW, the 4 nm Au wetting layer was physically deposited by an RF-sputter with the condition of 60 W RF-power at 1 mTorr pressure with 10 sccm gas flow rate for 4 s. As a consequence, Au grains were not fully connected together and, thus, started to become agglomerated and separated through the post-annealing process. During the RF-sputtering, AuNPs were deposited not only on the SiNW but also on the pad and substrate. AuNPs on the pad and substrate region could make the effective DNA concentration on SiNW lowered. Resultantly, the sensitivity would be decreased. However, the high enough sensitivity to detect 1 pM of DNA was attained in spite of disturbance by the AuNPs on the pad area. The size of pad is 100 μm × 100 μm, which is bulky compared to SiNW: a diameter of 50 nm and a length of 500 nm. The bulky region did not affect the measurement performed especially under dry atmosphere since its sensitivity is negligible. The final structure of GN embedded SiNW was identified by scanning electron microscopy images (SEM; FEI Sirion) AuNP.

2.2. Reagents

The GN embedded SiNW devices were immersed into a deionized (DI) water solution containing 10 μM of thiolated-probe oligonucleotides for 2 h and then rinsed with DI water. The coadsorption of the preimmobilised DNA oligonucleotide layers on the GNs was performed by 100 μM mercaptohexanol (Sigma–Aldrich) for 30 min to displace such unwanted probe oligonucleotides which were not adsorbed through the thiol end group and to put the fallen probe oligonucleotide back up. The mercaptohexanol treated devices were then hybridized with specific target oligonucleotides of the breast cancer DNA for 12 h. The sequence of 23-mer probe oligonucleotide, complementary, and non-complementary target oligonucleotides are as follows:

Probe DNA oligonucleotide: HS-5′-TTCGTTCATCACAATTTCGCCTT-3′ (Bioneer, Republic of Korea).
Complementary Target: 3′-AAGCAAGTAGTGTTAAAGCGGAA-5′ (Bioneer, Republic of Korea).
Non-complementary Target: 3′-GCTCGAAGAAGGATAAGAACGAA-5′ (Bioneer, Republic of Korea).

For the recovery test to assure the specific DNA binding, the complementary target oligonucleotide hybridized device was immersed in hot DI water (70 °C) for 8 min and rinsed several times.

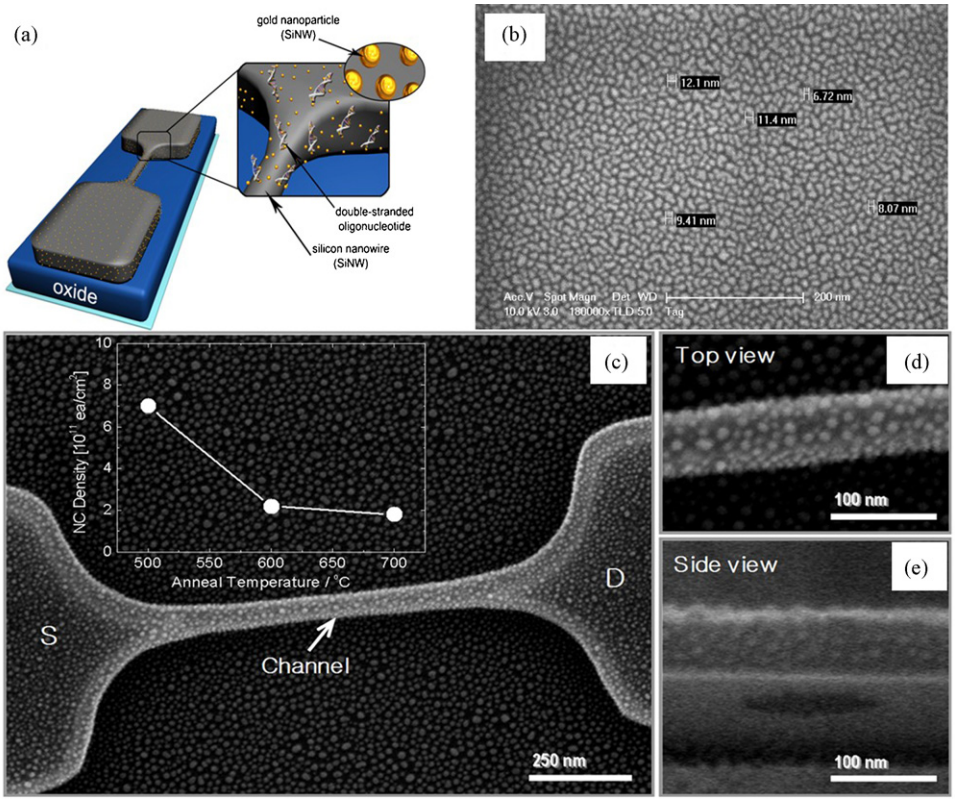

Fig. 1. (a) Schematic and (b)–(e) SEM images of the GN embedded SiNW device. (b) The cracked Au film due to incomplete agglomeration at 400 °C and (c) Au nanoparticles after complete agglomeration at 500 °C. The SEM close-up view at the top (d) and the side (e) of the SiNW.

2.3. Electrical measurement

The immobilization of the probe oligonucleotides and hybridization with the complementary target oligonucleotides were monitored by measuring the change in the electrical characteristics of the GN embedded SiNW device. Current–voltage (I–V) characteristics were measured by the semiconductor parameter analyzer (Agilent, HP4156C) and a probe station in air environment, *i.e.* dried atmosphere. The drain voltage was swept from 0 V to 5 V with the source grounded.

3. Results and discussion

Fig. 1 shows the schematic (Fig. 1(a)) and SEM images of the GN embedded SiNW device. Fig. 1(d) and (e) are the magnified SEM images in top and side channel region of Fig. 1(c), respectively. The GN density can be controlled by the annealing temperature, as depicted in the inset of Fig. 1(c). GN density was approximately 7×10^{11} cm^{-2} at 500 °C so that it contributed to enlarging the effective surface area. It is worthwhile to note that when the annealing temperature is lower than 500 °C, GNs were not properly formed as shown in Fig. 1(b). As shown in Fig. 1(e), the GNs were formed even on the sidewall channel because of the improved step coverage of the initial Au film by relatively high pressure sputtering.

For each stage of the oligonucleotide binding, the electric current (I_D) flows accordingly between the source and drain electrode with the drain voltage (V_D). I_D–V_D after each stage was plotted at Fig. 2(a). The device with the probe functionalized (10 μM) on the GNs resulted in a 5 nA drain current increment in comparison with I_D (5 nA) of initial device at V_D = 5 V. Furthermore, after the hybridization of the target oligonucleotides to the conjugated probe ones (1 pM), I_D additionally increased by 8.5 nA against only the probe oligonucleotide binding at V_D = 5 V. This drain current increment originated from the enhanced hole current density on the p-type SiNW surface induced by the negatively charged probe and the target oligonucleotides (Song et al., 2006). The conductance change by the target oligonucleotides was depicted in Fig. 2(b). 4 times larger conductance was observed by target oligonucleotides hybridization compared to probe oligonucleotides immobilization at V_D = 5 V. LOD was evaluated by lowering the concentration of target oligonucleotides, as shown in Fig. 2(c). Non-complementary target oligonucleotides were also used as a control group to investigate the feasibility of the GN embedded SiNW for DNA detection. For each concentration of the oligonucleotides, 20 devices were measured. At the target oligonucleotide concentration of 1 pM, the I_D after the hybridization is three times larger than I_D after the immobilization while no significant current change was observed in the case of the non-complementary control group. From the experimental data, the conductance change at 1 pM of DNA was comparable to previously reported result at the same DNA concentration (Gao et al., 2007). Therefore there is enough room to improve the LOD. In addition to the comparable LOD, AuNP embedded SiNW are more biocompatible compared to the SiNW. Au is known to be one of the most biocompatible materials. DNA can be easily and selectively immobilized on Au surface by use of thio-group without any complicated and tedious self-assembled monolayer (SAM) formation. This biocompatibility can give more degree of freedom in design and implementation of biosensors.

Furthermore, the recovery test to break up the linked bonding between the probe and target oligonucleotides was performed to confirm that the increment of I_D was caused by its specific binding. It should be noted that I_D returned to the initial value before the hybridization of the target oligonucleotides, *i.e.* it is almost the same as the I_D of the immobilized probe oligonucleotides, as shown in Fig. 2(a). From this result, it is concluded that the specific binding between the probe and target oligonucleotides enables the current modulation; thus, this GN embedded SiNW configuration is feasible as a biosensor for the label-free DNA detection.

To investigate this phenomenon, simulation was carried out with the aid of a commercialized SILVACO tool, which has been commonly used for device and process simulation for a metal-

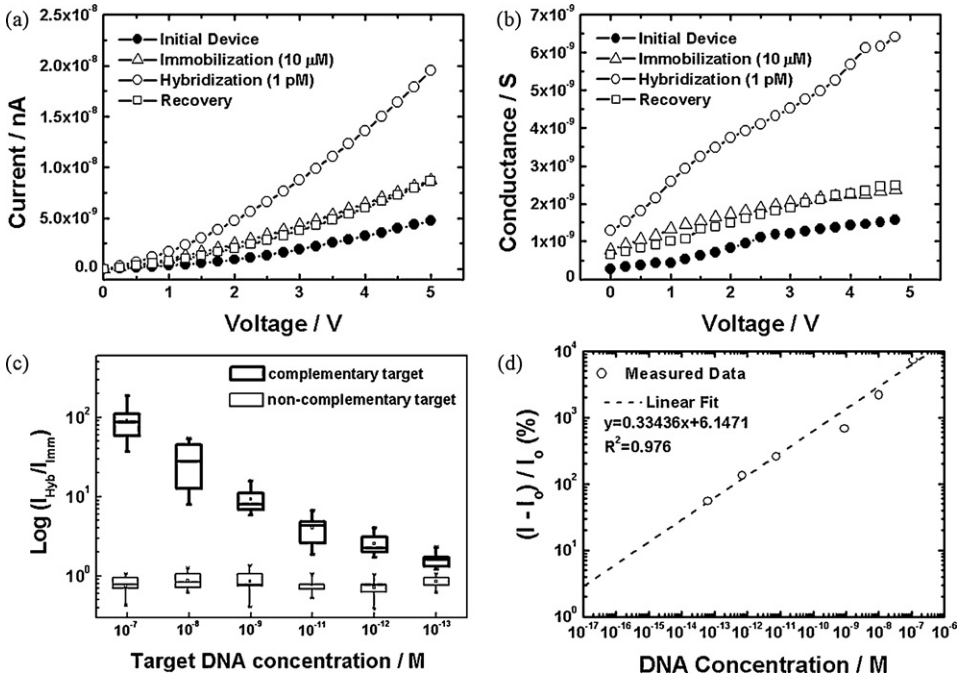

Fig. 2. (a) I_D–V_D characteristics of the GN embedded SiNW devices and (b) the conductance change without any adsorbate (filled-circle), with the probe oligonucleotides of 10 μM (hollow-triangle), and the complementary target oligonucleotides of 1 pM (hollow-circle), and after recovery treatment (hollow-square). (c) The current ratio of the complementary (solid box) and non-complementary (dashed box) target oligonucleotides' hybridization to the probe oligonucleotides' immobilization for the different target oligonucleotides' concentrations. (d) The calibration curve for LOD extraction.

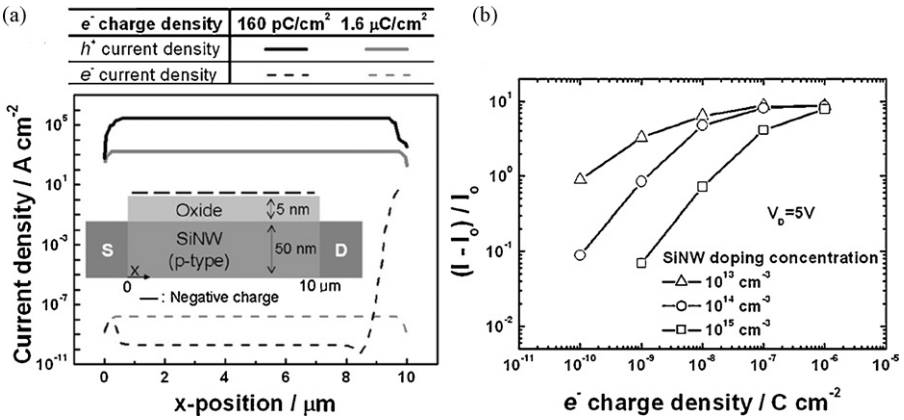

Fig. 3. (a) The simulated carrier density for hole (solid lines) and electron (dashed lines) for the different negative charge densities of 160 pC/cm^2 (gray lines) and 1.6 μC/cm^2 (black lines). (b) Current ratio dependency on the negative charge density for the different SiNW doping concentrations of 10^{13} cm^{-3} (triangle), 10^{14} cm^{-3} (circle), and 10^{15} cm^{-3} (square). I_{Qf} is the current with the negative charges, and I_{Fresh} is the current without the negative charge.

oxide-semiconductor field-effect-transistor (MOSFET) structure. The induced charges due to DNA hybridization were assumed to be interface charges, which played a role of traps in the oxide layer of SiNW. Simulated results show that the more negative charges in the range of 160 pC/cm^2 to 1.6 μC/cm^2, which intercalate to the probe and target oligonucleotides, raise the hole current density rather than the electron current density along the SiNW (Fig. 3(a)).

In Fig. 3(b), the current with the negatively charged (I_{Qf}) dependency on the negative charge density originating from the probe and target oligonucleotides was simulated for three different doping concentrations of 10^{13} cm^{-3}, 10^{14} cm^{-3}, and 10^{15} cm^{-3} to support sensitivity improvement for the suggested structure. Sensitivity improvement by reducing doping concentration was already reported by simulation (Nair and Alam, 2007) and experiment (Kim et al., 2007). The simulated structure is the same as that in the inset of Fig. 3(a). As the doping concentration decreases, the current ratio of the current with the negative charges (I_{Qf}) to the current without the negative ones (I_{Fresh}) increases at the fixed value of the negative charge density. Thus, further LOD improvement can be expected by reducing the device doping concentration.

4. Conclusion

The gold nanoparticle (GN) embedded silicon nanowire (SiNW) configuration was proposed, and its feasibility as well as sensitivity was demonstrated as the label-free DNA biosensor. After simple immobilization of oligonucleotides by virtue of the chemical affinity with thiol on the gold nanoparticles embedded silicon nanowire, the 23-mer complementary target oligonucleotides corresponding to the breast cancer DNA were detected at a 1 pM concentration. At high concentration (0.1 μM), the current was increased by 100 times after the specific binding of the conjugated oligonucleotides. For optimization of sensibility, the structure of the GN embedded SiNW was simulated, and it was confirmed that further enhancement can be expected by lowering the device doping concentration. Also, this simple DNA-biosensor configuration is highly attractive due to the high scalability and compatibility based on the conventional semiconductor technology as well as high sensitivity and potentially high thermal stability based on the spherical GN nanostructure.

Acknowledgements

This work was supported by the NRL Program of the Korea Science and Engineering Foundation (KOSEF) grant funded by the South Korean Government (MEST) (ROA-2007-000-20028-0 and ROA-2007-000-20127-0) and the National Research and Development Program (NRDP, 2005-01274) for the development of biomedical function monitoring biosensors, sponsored by the Korea Ministry of Science and Technology (MOST).

References

Akamatsu, K., Kimura, M., Shibata, Y., Nakano, S.-I., Miyoshi, D., Nawafune, H., Sugino, N., 2006. Nano Letters 6, 491–495.
Asano, K., Choi, Y.-K., King, T.-J., Hu, C., 2001. IEEE Transactions on Electron Devices 48, 1004–1006.
Caruso, F., Rodda, E., Furlong, D.N., 1997. Analytical Chemistry 69, 2043–2049.
Chehab, F.F., Kan, Y.W., 1989. Biochemistry 86, 9178–9182.
Drummond, T.G., Hill, M.G., Barton, J.K., 2003. Nature Biotechnology 21, 1192–1199.
Elfstrom, N., Karlstrom, A.E., Linnros, J., 2008. Nano Letters 8, 945–949.
Fritz, J., Baller, M.K., Lang, H.P., Rothuizen, H., Vettiger, P., Meyer, E., Guntherodt, H.-J., Gerber, C., Gimzewski, J.K., 2000. Science 288, 316–318.
Gao, Z., Agarwal, A., Trigg, A.D., Singh, N., Fang, C., Tung, C.-H., Fan, Y., Buddharaju, K.D., Kong, J., 2007. Analytical Chemistry 79, 3291–3297.
Homola, J., Yee, S.S., Gauglitz, G., 1999. Sensors and Actuators B 54, 3–15.
Kim, A., Ah, C.S., Yu, H.Y., Yang, J.-H., Baek, I.-B., Ahn, C.-G., Park, C.W., Jun, M.S., 2007. Applied Physics Letters 91, 103901.
Liu, S.-F., Li, Y.-F., Li, J.-R., Jiang, L., 2005. Biosensors & Bioelectronics 21, 789–795.
Lytton-Jean, A.K.R., Mirkin, C.A., 2005. Journal of The American Chemical Society 127, 12754–12755.
Nair, P.R., Alam, M.A., 2007. IEEE Transactions on Electron Devices 54, 12, 3400–3408.
Ohgi, T., Sheng, H.-Y., Nejoh, H., 1998. Applied Surface Science 130, 919–924.
Song, K.-S., Zhnag, G.-J., Nakamura, Y., Furukawa, K., Hiraki, T., Yang, J.-H., Funatsu, T., Ohdomari, I., Kawarada, H., 2006. Physical Review E 74, 041919.
Xu, J., Craig, S.L., 2005. Journal of the American Chemical Society 127, 13227–13231.
Yang, J., Yang, T., Feng, Y., Jiao, K., 2007. Analytical Biochemistry 365, 24–30.